Journal of Solid State Electrochemistry (2021) 25:2009–2020
https://doi.org/10.1007/s10008-021-04985-z

ORIGINAL PAPER

Investigations on Na-ion conducting electrolyte based on sodium alginate biopolymer for all-solid-state sodium-ion batteries

M. Infanta Diana[1] · P. Christopher Selvin[1] · S. Selvasekarapandian[1,2] · M. Vengadesh Krishna[2]

Received: 10 March 2021 / Revised: 3 May 2021 / Accepted: 30 May 2021 / Published online: 8 June 2021

Abstract

Herein, solid biopolymer electrolyte membranes based on sodium alginate are prepared and investigated for their application in sodium-ion batteries. Various concentrations of sodium thiocyanate (NaSCN) are introduced into the matrix of sodium alginate biopolymer. Solution cast route is the method opted to prepare the electrolyte membrane. The complex formation between sodium alginate and NaSCN has been confirmed with the help of X-ray diffraction (XRD) analysis and Fourier transform infrared spectroscopy (FTIR). On increasing NaSCN concentration, the semi-crystalline nature of the sodium alginate gets abated thus elevating the amorphous domain of the electrolyte membrane. Information about the glass transition temperature (T_g) is acquired from differential scanning calorimetry (DSC). Decrement in the T_g upon NaSCN addition favors the segmental motion of the polymer chain. The biopolymer host material (30 wt%) can accommodate large amounts of NaSCN salt (70 wt%) exhibiting ionic conductivity of 1.22×10^{-2} S cm^{-1}. The transference number measurement with Wagner's DC polarization method is found to be 0.96 (near unity) which confirms ions are the governing charge carriers. The linear sweep voltammetry (LSV) technique that measures the potential window for the biopolymer electrolyte membrane is 2.7 V, representing it as a potential applicant for electrochemical energy storage devices. An all-solid-state sodium-ion battery is assembled with a high ion–conducting biopolymer electrolyte membrane that displays an open cell potential of 2.87 V. The results highlight the possibilities of sodium ion–conducting solid biopolymer electrolytes to extend their hands in a safe sodium-ion battery.

Keywords Sodium thiocyanate · Ion conductivity · Glass transition temperature · Transference number

Introduction

Energy production and storage systems have been utilizing lithium-ion batteries (LIBs) to meet modern life's requisites and demand. But lithium's declining rate and increasing cost reduce its implementation on further developments on battery technology [1]. It is therefore important to increase the expansion of alternative energy storage systems capable of complementing the lithium-ion battery. Sodium (Na) is of immediate interest which is being studied owing to its high available resource, low cost, electrochemistry, and performances [2, 3]. Continuous pursuit of safe energy storage, batteries have enforced strict standards on aqueous electrolyte materials because of difficulties such as fluid leakage, feeble thermal stability, and ignitability. In this context, the solid electrolyte serves as an effective ion conductor and as a separator between the electrodes [4, 5]. A good electrolyte need to address two major challenges. One is to produce free-standing solid electrolyte with high ionic conductivity, and the other is to increase intimacy between solid electrolyte and the electrodes. Polymer-based solid electrolytes have been developed as a substitute for ceramic and liquid electrolytes in several electrochemical devices. It is also explored for its simplicity of operation, lightweight, greater reliability, and capacity to make effective electrode–electrolyte contact [6, 7]. Electrolytes based on polyethylene oxide (PEO) are most intensively studied due to their high solvent power and complexation [8]. Other common polymers such as polyethylene glycol (PEG) [9], polyvinylpyrrolidone (PVP) [10], polycarbonate [11], and poly(ionic liquid) [12] have also been investigated.

✉ P. Christopher Selvin
csphysics@buc.edu.in

[1] Luminescence and Solid State Ionics Laboratory, Department of Physics, Bharathiar University, Coimbatore 641046, India

[2] Materials Research Center, Coimbatore 641045, India

Introducing alkali metal salt into the matrix of the polymer is one of the significant methods in augmenting ion conduction of the polymer electrolytes [13]. The polymer host and metal salt combination complement each other by providing mechanical stability and ion conduction respectively. During polymer-salt interaction, the ions from the salt coordinate with the polar groups of polymers altering the crystalline/amorphous nature of the membrane. The addition of salt disturbs the hydrogen bonding between the polymer chains which improves the amorphous phase of the polymer electrolyte thereby providing an ion conduction pathway [14–16].

On the other hand, the mounting "white pollution" threat insists on the exploration of biodegradable materials. Many such materials excel in the field of energy storage, which has brought polysaccharides to the front as promising eco-friendly biopolymers [17]. These materials can be discarded and reused by utilizing relatively inexpensive methods with very low environmental effects. Biopolymers emerge from ample, cost-effective, and leak-free natural resources. Copious investigations have been conducted based on natural biopolymers for several electrochemical applications [18–22]. It is perceived that the material's structures ought to be flexible that they can provide accommodation for larger ions such as Li^+ and Na^+, without any hindrances and to participate in faster diffusion kinetics. In this scenario, finding a host material with functional diversity is of greater importance. The host material should ideally fulfill few requirements, such as a high degree of amorphicity, the high segmental motion of polymer chains, and poor coordination of ions that enables the ions to jump between polymer's coordinating sites [23].

Recently, membranes based on sodium alginate (SA) biopolymers have been proposed. Sodium alginate is a polymeric material of carbohydrate group that originates from the membrane of brown algae cell, which has been widely used in the food and tissue engineering industry due to its biodegradability and sustainability [24, 25]. Supportively, sodium alginate has also found its application as binders in Li-ion batteries particularly for anode materials [26]. Development in the field of energy storage devices with alginate-based membranes is at its early stage, and hence, it is promising to explore its properties and applications [27, 28]. The alginate polymer is an anionic polysaccharide with a rigid polymer chain, composed of two uronic acids. One is α-D-mannuronic acid (M-block) and the other one is β-L-guluronic acid (G-block), which is bound together by a glycoside connection as shown in (Fig. 1). Since alginate is rich in oxygen atoms, they can form a coordinate bond with cations [29]. Furthermore, sodium alginate exhibits standard film properties such as high solubility, flexibility, non-toxicity, and biocompatibility which are highly preferable for solid-state electrolyte systems [30]. Among the inorganic cations, ambidentate SCN^- is most popular due to its tendency for association/dissociation with metal ions [31, 32].

To improve the ionic conductivity, efforts have been made to obtain a polymeric matrix with reduced crystallinity and low glass transition temperature. The development of a novel sodium ion-conducting biopolymer electrolyte membrane based on water-soluble sodium alginate is reported in this work for the first time for exploring its application in sodium-ion batteries. Several trials have been made by incorporating NaSCN into sodium alginate to optimize the ideal concentration for obtaining a highly ion-conductive biopolymer electrolyte.

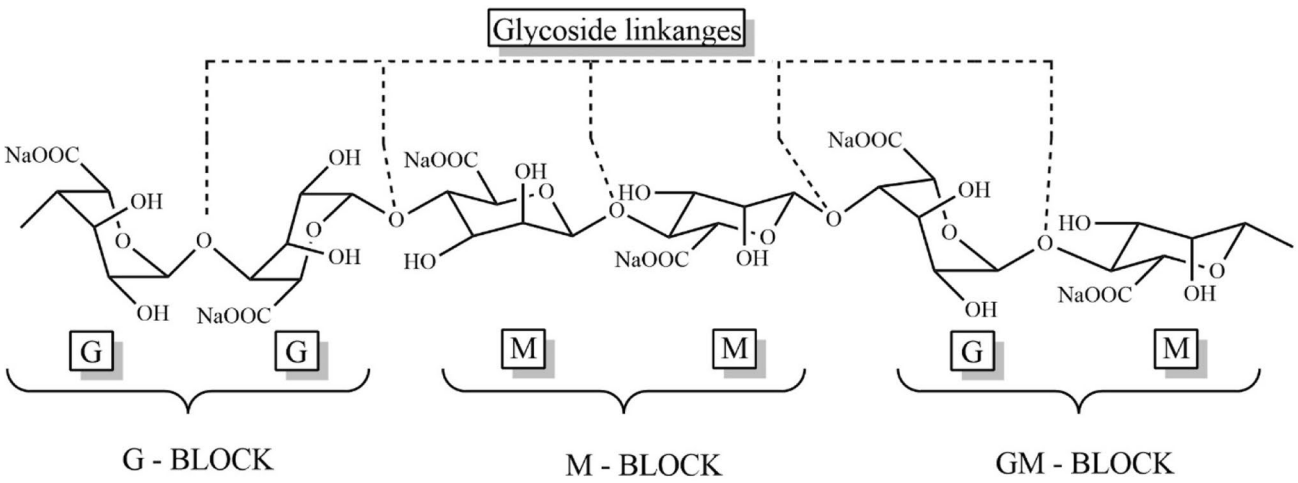

Fig. 1 Structure of sodium alginate

Experimental method and instrumentation

Materials and biopolymer electrolyte preparation

In the present work, sodium alginate with molecular weight 216.12 g/mol from SD Fine Chem Limited and sodium thiocyanate (NaSCN) with molecular weight 81.072 g/mol from Sisco Research Laboratories (SRL) are used to prepare sodium ion-conducting polymer electrolyte membranes using deionized water as solvent. Membranes with various molecular weight percentage (wt%) of sodium alginate and NaSCN (70:30, 60:40, 50:50, 40:60, 30:70, 20:80 sodium alginate: NaSCN) are prepared. The sodium alginate powder is first dissolved in 50 ml of deionized water at 90 °C. Then, the solution is stirred for several hours until it becomes a clear viscous solution. Subsequently, NaSCN (30–80 wt%) is added to the sodium alginate solution which is vigorously stirred for 1 h to obtain a homogenous solution. Pure sodium alginate membranes without complexing with NaSCN are also prepared. Later, the solutions are cast into polypropylene petri dishes and dried in a hot air oven at 70 °C for 12 h. Freestanding membranes with a thickness of 200 µm have been obtained and stored in a vacuum desiccator for analysis.

Bio-polymer electrolyte characterization

Prepared biopolymer membranes (100:0, 70:30, 50:50, 30:70, 20:80 wt% of sodium alginate: NaSCN) are subjected to various characterization techniques. The crystalline/amorphous nature of the membranes is examined by XRD-Rigaku Ultimate IV Japan. X-rays of wavelength 1.541 Å generated by the Cu-K_α source. The FTIR measurement is performed by Thermo Scientific Nicolet IS10 and recorded in the transmittance mode at room temperature. Differential scanning calorimetry (DSC) is measured through TA Instruments DSC Q20 V24.10 Build 124 to understand about thermal properties of biopolymer electrolyte membranes. To determine the ionic conductivity of the electrolyte membrane, AC impedance spectroscopy is used. The electrolyte film is placed between stainless steel electrodes to measure the impedance using HIOKI 3532 LCZ HiTESTER (frequency range of 42 Hz–5 MHz). The transference number measurement for the high ion-conducting electrolyte membrane is evaluated using Wagner's DC polarization method. The working potential window of the biopolymer electrolytes is analyzed by linear sweep voltammetry measurements via a two-electrode system with the scan rate of 5 mVs^{-1} using BioLogic SP-150.

Battery fabrication

For the preparation of electrodes, sodium metal blocks, MnO_2 (molecular weight 86.937 g/mol), and graphite powder are purchased and used as received. A thin sodium metal layer (0.05 cm in thickness) is stripped from sodium metal blocks and used as an anode. The composite powder of manganese dioxide (MnO_2) and graphite (3:1 ratio) is pelletized (2 cm in diameter) with the pressure of 5-Torr and used as cathode. The high ion-conducting sodium alginate biopolymer membrane is sandwiched between the anode and the cathode. The cell with [Na metal | biopolymer electrolyte | MnO_2 + Graphite] configuration is assembled in a stainless steel battery holder. The open-circuit potential and the discharge profile of the cell are observed through this arrangement.

Results and discussion

X-ray diffraction analysis

The XRD analysis of sodium alginate-NaSCN complexes is performed to investigate the impact of NaSCN inclusion on sodium alginate–based biopolymer electrolyte membrane. Figure 2a represents the diffractogram of uncomplexed sodium alginate and NaSCN complexed sodium alginate. The broad semi-crystalline peaks at 13.12° and 23.34° attribute to the typical polysaccharides in sodium alginate polymer membrane which is in good agreement with Yang et al. [28]. The incorporation of NaSCN produces changes in the polymer's crystalline/amorphous nature. Characteristic peaks of sodium alginate shift to 14.36º and 23.80º with changes in intensity. Figure 2b gives a clear comparative picture of prepared biopolymers. The appearance of NaSCN peak at 44.12º (JCPDS card no. 70–0946) is realized with 30 wt% NaSCN inclusion on 70 wt% sodium alginate [33]. A new amorphous halo at $2\theta \sim 26º$ is observed upon the addition of 50 wt% NaSCN, and the peak corresponding to NaSCN disappears indicating the complete dissolution of the salt. As NaSCN interacts with the coordinating sites of the polymer, it disrupts the bonding between the polymer chains which suppresses its crystalline nature [14, 34, 35]. The coordination of Na ions with the hydroxyl groups of the polymer main chain has a significant impact on the mobility and microstructure of the polymer chain [15]. Subsequently, the amorphous phase of the biopolymer electrolyte is improved which is realized from the broadness of the peak [36, 37]. A high degree of amorphicity is observed with 70 wt% NaSCN concentration in 30 wt% sodium alginate backbone. The halo gets shifted and becomes more prominent at 31.46º. This shift is an indication of the amorphous phase due to the formation of polymer salt complexes [38, 39]. A similar trend is observed in sodium alginate-NH_4Br complexes [40]. As the polymer membrane becomes more amorphous, there is an opportunity for reduction in energy barriers for the polymer chains which is one of the most favorable conditions for ionic transport [41, 42].

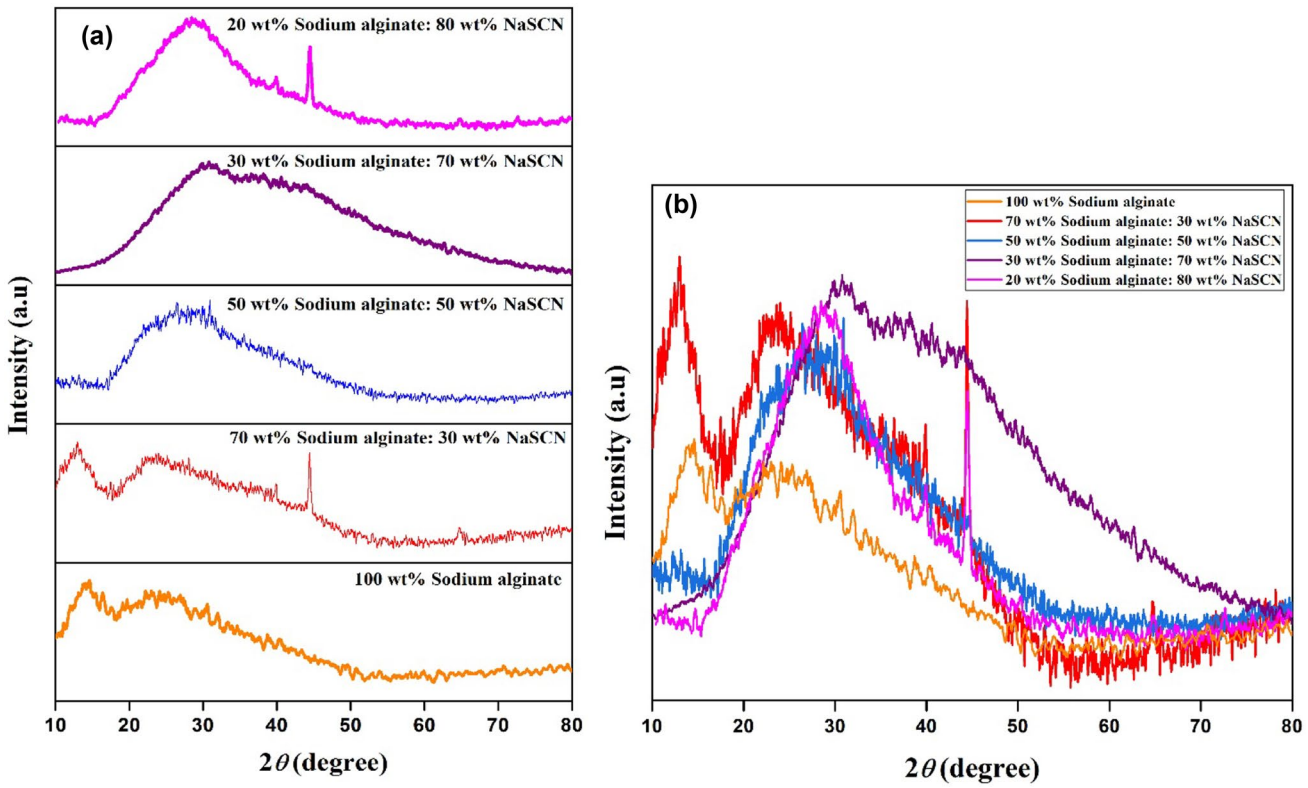

Fig. 2 **a** XRD patterns of uncomplexed sodium alginate and various compositions of sodium alginate-NaSCN complex. **b** Comparative XRD patterns of prepared biopolymer electrolytes

To support the outcome, the degree of crystallinity has been calculated by the following equation:

$$X_C = A_c/(A_c + A_a) \times 100\%$$

The area under the crystalline peak and the amorphous peak has been integrated and used. The obtained percentage is shown in Table 1. It establishes the degree of crystallinity of the sample decreases with an increase in NaSCN concentration. This variation in the degree of crystallinity of the polymer membrane is concomitant with the breakage of polymeric bonds, which leads to a disordered state of the membrane. The increase in disorders may lead to an enhancement of the free-volume content [15]. Although the increase in NaSCN content into the polymer site is beneficial, the polymer host is incapable of accommodating more sodium ions beyond 70 wt% NaSCN. The appearance of NaSCN peak and increased intensity approves the formation of ion aggregation which may be due to reduced solubility, poor complexation, and reforms in polymer chains [43]. Thus, XRD analysis aids to identify and scrutinize the optimal concentration (70 wt% of NaSCN) for procuring an enhanced amorphous phase.

Table 1 Degree of crystallinity of prepared biopolymer electrolyte membranes

Sodium alginate/NaSCN composition (wt%)	Degree of crystallinity (X_C)
100:0	48.36%
70:30	27.81%
50:50	23.74%
30:70	18.48%
20:80	62.68%

FTIR analysis

An effective tool to examine the complex formation between biopolymer sodium alginate and NaSCN is the FTIR technique. The FTIR spectra of uncomplexed sodium alginate polymer membrane and the polymer membranes with various compositions of sodium alginate and NaSCN are shown in Fig. 3. The peaks at 1100 cm^{-1}, 1395 cm^{-1}, 1640 cm^{-1}, 2934 cm^{-1}, and 3393 cm^{-1} are due to glycoside bond (C–O–C), symmetric stretching of (COO^-), asymmetric stretching of (COO^-), and CH stretching and stretching vibrations of OH groups present in the sodium alginate polymer respectively [44]. On NaSCN incorporation, a shift in the absorption peaks with changes in intensity is observed which approves the attraction between ionic salt

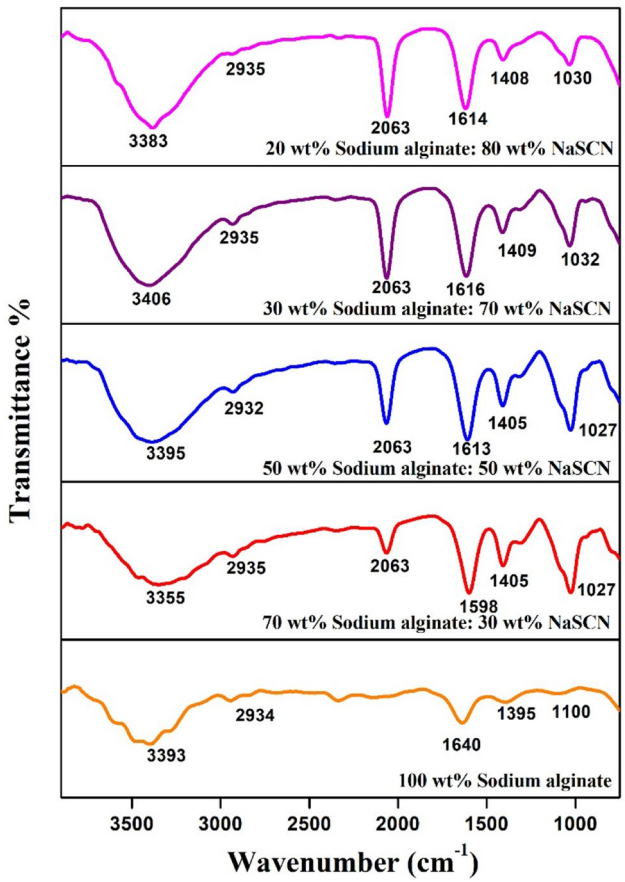

Fig. 3 FTIR spectra of uncomplexed sodium alginate and various compositions of sodium alginate-NaSCN complex

and the lone pair of electrons of the polymer [45, 46]. The appearance of a new peak at 2063 cm^{-1} is observed for all the complexed membranes which are due to SCN^- stretching [47]. An increase in NaSCN concentration increases the possibility of ion dissociation with a high chance of cation getting complexed with the coordinating sites of the polymer [48]. The FTIR peak positions and their corresponding vibrational assignments for all the biopolymer membranes are given in Table S1. The peak at 3393 cm^{-1} is due to OH groups of polysaccharides, which gets shifted to 3355 cm^{-1}, 3395 cm^{-1}, 3406 cm^{-1}, and 3383 cm^{-1} on NaSCN addition. The changes in the intensity and the broadness of the OH band for the sodium alginate complexed system may be due to the disturbances in the OH band [45]. With the intensification of NaSCN concentration in the sodium alginate system, CH stretching at 2934 cm^{-1} has no much effect on NaSCN additon on NaSCN addition, which reveals that it retains strong bonding with polymer backbone. Similar observations have been reported by A.F Fuzlin et al. [44]. The peak which corresponds to the glycoside bond (C–O–C) of sodium alginate shows minor shifts at 1027 cm^{-1} with 30 and 50 wt% inclusion of NaSCN. Increasing its concentration to 70 wt% in 30 wt% sodium alginate peak gets shifted to higher wavenumber 1032 cm^{-1}. This may be due to the perturbations in the C–O–C functional group because of the interaction between cation with the ether oxygen of the polymer chain. Another significant peak that attributes to asymmetric stretching of (COO^-) of sodium alginate at 1640 cm^{-1} gets shifted to 1598 cm^{-1}, 1613 cm^{-1}, 1616 cm^{-1}, and 1614 cm^{-1} with increasing NaSCN content. The symmetric COO^- stretching observed at 1395 cm^{-1} shifted to 1405 cm^{-1}, 1405 cm^{-1}, 1409 cm^{-1}, and 1408 cm^{-1}. Figure 4 depicts the possible interactions between the functional group of the polymer and NaSCN. The changes in the vibrational frequencies of OH, COO^-, and C–O–C groups of sodium alginate validate the interaction with the Na^+ ions of NaSCN via intramolecular interactions. Furthermore, the functional groups of different sodium alginate chains also interact intermolecularly with the Na^+ ions of NaSCN consequently ending up in complex formation [49]. All these vibrational shifts indicate the occurrence of salt-polymer interaction at the polar groups via weak Van der Waals attraction [50, 51]. Thus, FTIR investigation gives a clear sign about the complexation between sodium alginate—NaSCN.

DSC analysis

The glass transition temperature is a key performance indicator since it defines the flexibility and mobility of the chain segmental motion (which helps in ion migration) [11]. The glass transition temperature (T_g) and melting temperature (T_m) of the biopolymer electrolyte membrane are obtained by performing DSC analysis. Figure 5 shows the DSC thermograms of biopolymer electrolyte membranes. Uncomplexed sodium alginate showed a broad T_g value at 52.51 °C which is found to be low when compared with other literatures [52, 53]. This may be due to the dissemination of the molecular weight, chain length, and crosslinks of the polymer membrane. Sodium alginate is a polysaccharide polymer comprising two hydroxyl segments and one carboxylate segment that forms very strong inter and intramolecular hydrogen bonding. The incorporation of salt would affect the hydroxyl and carboxylate segments [54]. On NaSCN addition (30 wt%), T_g value gets decreased to 49.88 °C. With 50 wt% of salt,

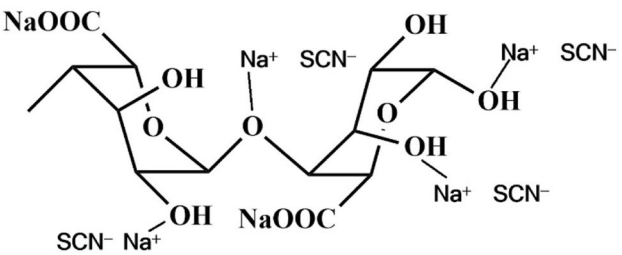

Fig. 4 Possible interactions between sodium alginate and NaSCN

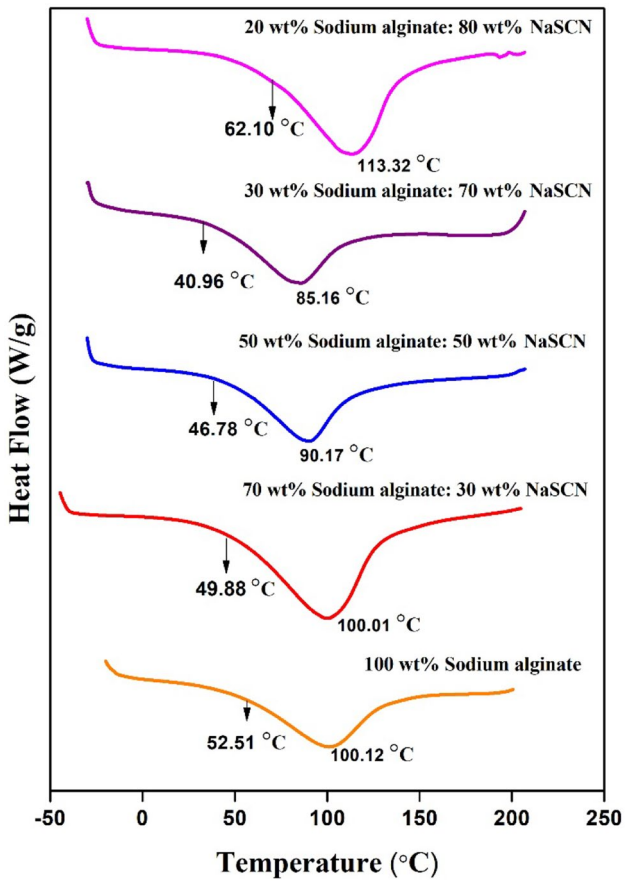

Fig. 5 DSC thermograms of uncomplexed sodium alginate and various compositions of sodium alginate-NaSCN complex

T_g further decreases to 46.78 °C which may be due to the plasticizing effect of the salt concerning the concentration of coordinating segment of sodium alginate. The concentration of the carboxylate segment has a substantial influence on T_g [53]. The inclusion of NaSCN lowers the viscosity which proliferates the distance between the polymer chains and its segmental motion resulting in a lower T_g value [55]. Since low T_g value is highly associated with high polymer flexibility, it helps in softening of the polymer matrix making it more flexible [11, 56]. Biopolymer membrane with 70 wt% of NaSCN showed the lowest T_g value of 40.96 °C. As the addition of salt exceeding threshold concentration, T_g gets increased to 62.10 ℃ which is due to the creation of ionic cross-linkages between dissociated salt and the polymer chain segments. The cross-linkage impedes the movement of polymer segments thereby elevating its energy barrier, crystalline phases, and polymer hardness [11]. Table 2 comprises the values of T_g and T_m for all the biopolymer membranes. The DSC investigations are in accordance with the XRD results where 70:30 wt% of sodium alginate and NaSCN showed high amorphous phases, exhibit low T_g value. Thus obtaining an amorphous polymer domain with a low glass transition temperature would improve the polymer's flexibility and segmental motion [53]. This flexible backbone of the polymer may harvest fast ion conductions.

Table 2 Glass transition temperature and melting temperature of prepared biopolymer electrolyte membranes

Sodium alginate/NaSCN composition (wt%)	Glass transition temperature (T_g)	Melting temperature (T_m)
100:0	52.51 ℃	100.12 ℃
70:30	49.88 ℃	100.01 ℃
50:50	46.78 ℃	90.17 ℃
30:70	40.96 ℃	85.16 ℃
20:80	62.10 ℃	113.32 ℃

AC impedance analysis

The Nyquist plots (Z' vs $-Z''$) of uncomplexed sodium alginate membrane and sodium alginate-NaSCN complexes are shown in Fig. 6a, b. The measurements are carried out with stainless steel electrodes at room temperature (303 K). The complex plot of the sodium alginate membrane shows two well-defined regions: the depressed semicircle at high-frequency region and a spike at low-frequency region. The semicircle appearance may be due to the migration of Na^+ ions in the bulk of the biopolymer electrolyte membrane [57]. Meanwhile, immobile polymer chains get polarized due to the altering field current which is realized as a double-layer capacitor or constant phase element (non-ideal capacitor). Hence, the depressing semicircle can be represented by the parallel combination of bulk resistance and bulk capacitance of the polymer. Since stainless steel blocking electrodes are used to measure the frequency response, charges at the interface will tend to accumulate [58]. The low-frequency inclined spike indicates the polarization of charges (capacitive behavior) at the electrode/electrolyte interface [59]. The equivalent circuit which fits the complex impedance is shown as an inset in Fig. 5. The bulk resistance R_b of the electrolyte membrane is extracted from the EQ software program which is developed by B.A. Boukamp [60]. The ionic conductivity is calculated using the following equation:

$$\sigma = l/R_b A \qquad \left(Scm^{-1}\right)$$

where l is the thickness of the electrolyte, R_b is the bulk resistance, and A is the area of the electrolyte membrane. Ionic conductivity for uncomplexed sodium alginate is found to be 7.65×10^{-6} S cm^{-1}. Incorporating NaSCN, the diameter of the semicircle gets reduced which results in reduced bulk resistance of the membrane. Similar observations are noted when the concentration of the salt increases the ionic conductivity from 7.65×10^{-6} to 1.44×10^{-4} S cm^{-1} for

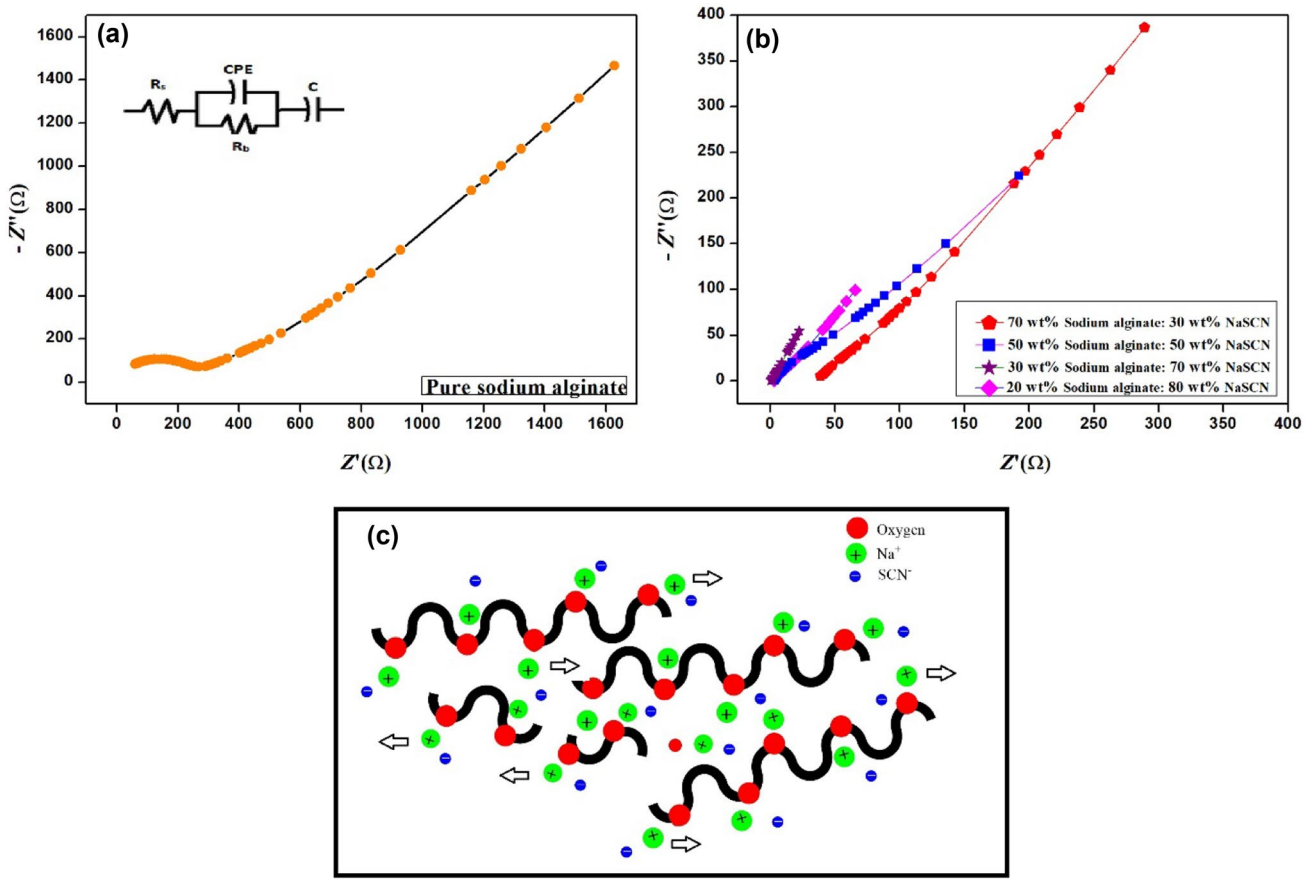

Fig. 6 **a** Nyquist plot of uncomplexed sodium alginate. The inset figure represents the equivalent circuit. **b** Nyquist plot of various compositions of sodium alginate-NaSCN complex. **c** Schematic diagram of Na + migration pathways in polymer matrix

70:30 wt% of sodium alginate and NaSCN membrane. It is expected that the ionic conductivity of sodium alginate-NaSCN depends on the degree of crystallinity as well as the concentration and mobility of the polymer chains carrying the charge carriers [49]. When SCN^- anion is bounded with its coordinating site, ion-ion interactions get avoided, increasing the dissociated Na ions (charge carriers). Upon electric field application, weakly coordinated Na^+ ions move from the polymer coordination site which is accountable for the transport properties. Essentially, the amorphous phase appearing in the highly concentrated salts pave the way for the conduction of ions [14]. Because ionic migration which arises at the amorphous phase of the material contains local free volume which acts as conduction pathways for ions [14, 49]. And therefore, ionic conductivity gets improved to 4.13×10^{-3} S cm^{-1} when 50 wt% NaSCN is added. The biopolymer membrane with 70 wt% of NaSCN exhibits an excellent ionic conductivity of 1.22×10^{-2} S cm^{-1}. Table 3 displays the variation of ionic conductivity with increasing NaSCN concentration. The ionic conductivity increases with increasing concentration of NaSCN in the polymer matrix until it reaches a saturated value (70 wt% of NaSCN). And also, the increase is mainly related to the excess number of mobile charge carriers in the system. The conduction occurs via the hopping of Na^+ ions from the trapping centers (amorphous regions).

The transport of Na^+ ions is possible by the segmental motion with a charge carrier in its chain (Fig. 6c). As a result, higher ionic conductivity in the polymer membrane is observed because of the segmental motion within the amorphous phase. The conductivity drops to 2.33×10^{-4} S cm^{-1} beyond 70 wt% NaSCN. Once the ion-ion interaction gets increased, the ion aggregation and chain

Table 3 Ionic conductivity (σ) of prepared biopolymer electrolyte membranes

Sodium alginate/NaSCN composition (wt%)	Conductivity (S cm^{-1})
100:0	7.65×10^{-6}
70:30	1.44×10^{-4}
50:50	4.13×10^{-3}
30:70	1.22×10^{-2}
20:80	2.33×10^{-4}

mobility constraint reduce the number of mobile charges. A recent study on sodium ion-conducting polymer blend electrolyte membranes based on chitosan/dextran biopolymers has shown conductivity of 6.10×10^{-5} S cm^{-1} [14]. Ionic liquid-based cellulose derivative bio-sourced polymer electrolytes have exhibited ionic conductivity of $(4.54 \pm 1.2) \times 10^{-3}$ S cm^{-1} [61]. It is plausible from the present investigation that enhancement in the amorphous phase and segmental motion is highly correlated with ionic conductivity since they are responsible for easy and significant ion migration.

Transference number measurements

Another important parameter to define an electrolyte membrane as a good ionic conductor is its transference number [11]. The ionic transference number (t_{ion} of the mobile species in biopolymer electrolyte membrane is evaluated by Wagner's DC polarization method [62]. The current due to polarization is observed as a function of time on the application of DC potential (1.5 V) across the cell configuration: [stainless steel (SS) | biopolymer electrolyte | stainless steel (SS)] at room temperature. The total ionic transference number is calculated from the following equation:

$$t_{ion} = (I_f - I_i)/I_i$$

where I_i is the initial current and the I_f is the final current. When a small DC voltage is applied across the cell, due to the migration of ions, current starts to flow. This current gets polarized which results in high internal resistance [44]. As the number of mobile ions gets ceased, only the residual current persists. Figure 7 depicts the variation of polarization current to time for electrolyte membrane with 30:70 wt% of sodium alginate-NaSCN. The ionic transference number (t_{ion}) of highest conducting biopolymer membrane is found to be 0.96. It is observable from AC impedance analysis that sodium alginate membrane exhibited high ion-conductivity gives a glimpse about Na^+ participation as charge carriers. The movement of sodium ions may inhibit very high transference number which is also the result of negligible cation–anion interaction. The ionic transference number for the CMC-and $NaCH_3COO$ film is found to be 0.98 [61]. In another recent work of Okamoto et al. the Na^+ ion transference number of binary mixtures of $NaN(SO_2F)_2$ (NaFSA) and sulfolane (SL) is found to be as high as 0.8. The Na^+ ions interchange the ligands (solvent and anion) in the liquids which significantly affects the Na^+ ion transport under an anion-blocking condition [63]. Thus, the evaluation implies that Na-ions are predominant which supports the charge transport in the biopolymer system.

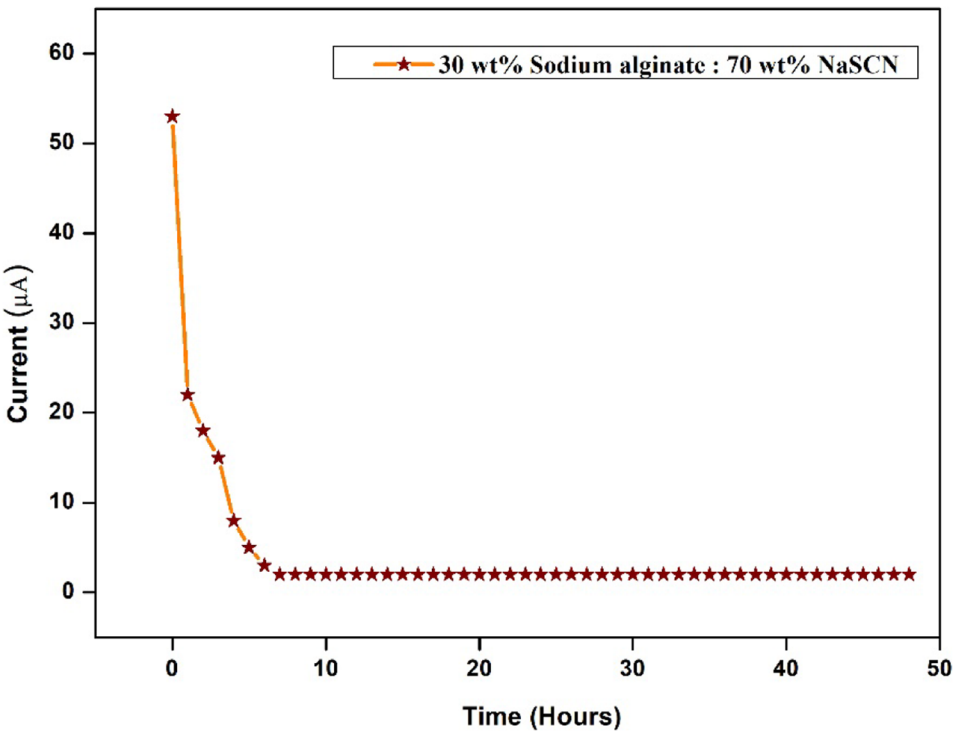

Fig. 7 Variation of polarization current with time for the high ion-conducting biopolymer electrolyte system (30 wt% sodium alginate: 70 wt% NaSCN) at room temperature

Linear sweep voltammetry

Linear sweep voltammetry (LSV) is performed to obtain an insight into the stability of the biopolymer electrolyte membrane using a two-electrode system, and the resulting voltammogram is shown in Fig. 8. As the potential is swept from 0 V toward the positive voltage with a scan rate of 5 mVs^{-1}, the current flow starts at a potential of 1.9 V, and the current gets a sudden upsurge. The onset current in the high voltage region is the result of the decomposition of the membrane [64]. Thus, the onset voltage of 2.7 V is taken as the upper limit to define the electrolyte stability. Likewise, Ibrahim et al. have reported a decomposition voltage of 1.8 V for sodium iodide incorporated in castor oil–based polyurethane [65]. Saiful et al. have shown electrochemical stability of $NaCH_3COO$ complexed carboxymethyl cellulose is 2.8 V [61]. An analysis by Isa et al. with polyvinylidene fluoride-co-hexafluoropropylene (PVDF-HFP)-sodium trifluoromethane sulfonate ($NaCF_3SO_3$) system accomplished potential stability of 3.4 V [66]. The present work shed a ray of anticipation for utilizing and developing the biopolymer electrolyte membrane for sodium-ion batteries.

Fabrication of solid-state sodium battery

The indicators of a perfect electrolyte membrane for extending its performance in battery applications are high ionic conductivity, high amorphous nature, undisrupted segmental motion, and unit transference number [11]. Hence, biopolymer membrane exhibiting the aforementioned properties is used for fabricating Na ion battery. A solid-state sodium ion-conducting primary battery is constructed with Na metal anode and (MnO_2 + Graphite) cathode which is separated by the biopolymer electrolyte membrane (30:70 wt% of sodium alginate and NaSCN). The open-circuit potential (OCP) of 2.87 V is observed and when the cell is discharged through the load of 100 KΩ, the voltage gets dropped to 1.7 V which may be due to the effect of electrode–electrolyte interface polarization [67]. The cell can fetch 1.7 V for 250 h (observed). Figure 9a, b depicts the photograph of the constructed battery and the discharge profile of the sodium-ion battery. The performance of the cell assembly establishes the suitability of the prepared biopolymer electrolyte membrane for its application in sodium-ion batteries.

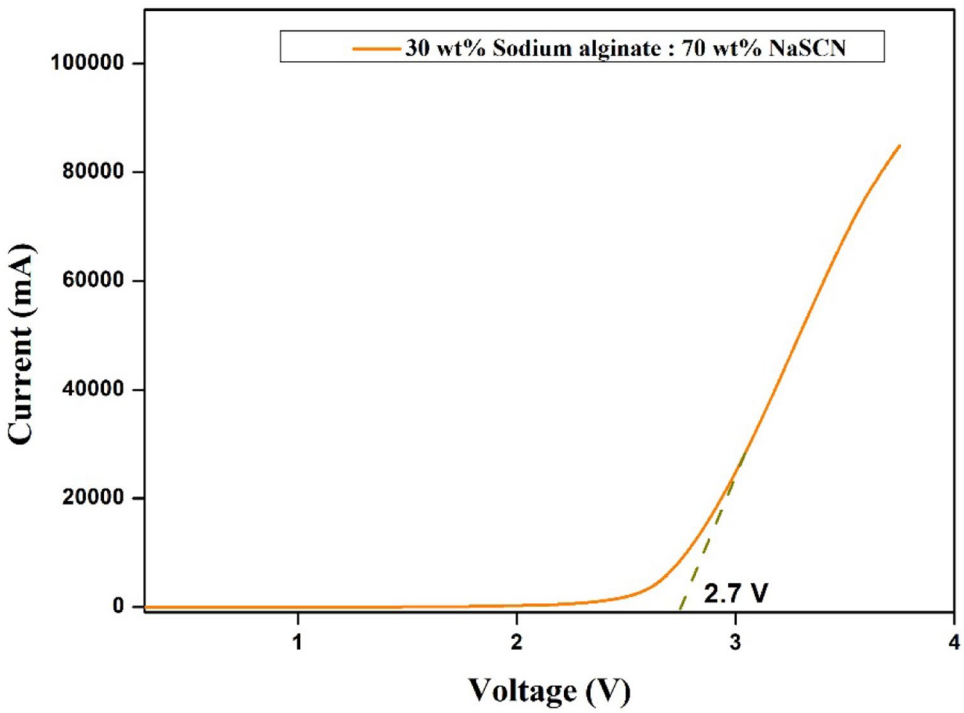

Fig. 8 Linear sweep voltammetry recorded for the high ion-conducting biopolymer electrolyte system (30 wt% sodium alginate: 70 wt% NaSCN)

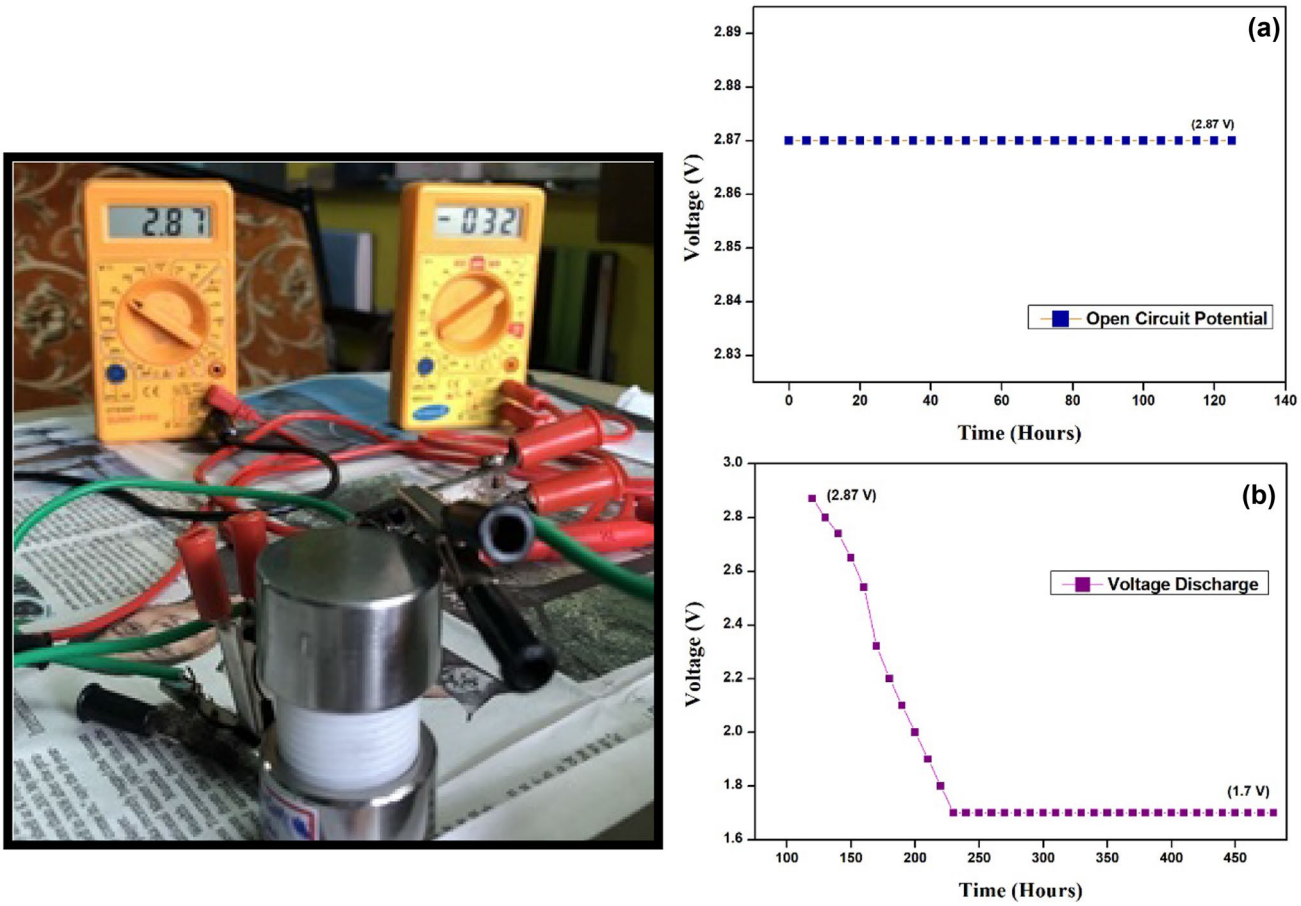

Fig. 9 Photograph of the fabricated battery displaying OCP of 2.87 V (left). **a** Open circuit potential of sodium battery with the high ion-conducting biopolymer membrane (30 wt% sodium alginate and 70 wt% NaSCN). **b** Discharge profile of sodium battery with function of time

Conclusion

For the first time, a novel combination of sodium alginate and NaSCN is examined and analyzed as an electrolyte membrane for a sodium ion-conducting battery. Membranes with various compositions of sodium alginate and NaSCN are prepared by the simple solution casting technique. The inclusion of NaSCN concentration has an effect on crystalline/amorphous nature, vibrational and thermal behaviors, and also on ion conduction properties. The XRD analysis unveils the utilization of optimal concentration in enhancing the amorphous nature of the polymer electrolyte membrane. The complex formation between sodium alginate and NaSCN has been confirmed by FTIR analysis. The polymer chain's segmental motion coupled with high amorphous nature, weaker Na^+-polymer chain coordination, and ion transference number near unity are the significant features in achieving high ionic conductivity. The biopolymer electrolyte membrane with 70 wt% NaSCN concentration in 30 wt% sodium alginate exhibits a conductivity of 1.22×10^{-2} S cm^{-1}. Sodium alginate's ability to accommodate a large amount (70 wt%) of NaSCN is notable in attaining exceptionally high ionic conductivity at room temperature (303 K), and it displays an open circuit potential of 2.87 V. In the quest for safe and reliable energy storage systems, sodium alginate-NaSCN electrolyte membrane possesses upright potential which unlocks great possibilities for sodium batteries.

Supplementary information The online version contains supplementary material available at https://doi.org/10.1007/s10008-021-04985-z.

Declarations

Competing interests The authors declare no competing interests.

References

1. Vikström H, Davidsson S, Höök M (2013) Lithium availability and future production outlooks. Appl Energy 110:252–266
2. Yabuuchi N, Kubota K, Dahbi M, Komaba S (2014) Research development on sodium-ion batteries. Chem Rev 114:11636–11682

3. Palomares V, Serras P, Villaluenga I, Hueso KB, Carretero-González J, Rojo T (2012) Na-ion batteries, recent advances and present challenges to become low cost energy storage systems. Energy Environ Sci 5:5884–5901
4. Che H, Chen S, Xie Y, Wang H, Amine K, Liao XZ, Ma ZF (2017) Electrolyte design strategies and research progress for room-temperature sodium-ion batteries. Energy Environ Sci 10:1075–1101
5. Kim JJ, Yoon K, Park I, Kang K (2017) Progress in the development of sodium-ion solid electrolytes. Small Methods 1:1700219
6. Farrington GC, Dunn B (1982) Divalent beta″-aluminas: high conductivity solid electrolytes for divalent cations. Solid State Ionics 7:267–281
7. Song S, Duong HM, Korsunsky AM, Hu N, Lu L (2016) A Na^+ superionic conductor for room-temperature sodium batteries. Sci Rep 6:1–10
8. Koduru HK, Iliev MT, Kondamareddy KK, Karashanova D, Vlakhov T, Zhao XZ, Scaramuzza N (2016) Investigations on poly (ethylene oxide) (PEO) - blend based solid polymer electrolytes for sodium ion batteries. J Phys Conf Ser 764:1–10
9. Manoravi P, Selvaraj II, Chandrasekhar V, Shahi K (1993) Conductivity studies of new polymer electrolytes based on the poly(ethylene glycol)/sodium iodide system. Polymer 34:1339–1341
10. Naresh Kumar K, Sreekanth T, Jaipal Reddy M, Subba Rao UV (2001) Study of transport and electrochemical cell characteristics of PVP:$NaClO_3$ polymer electrolyte system. J Power Sources 101:130–133
11. Mindemark J, Mogensen R, Smith MJ, Silva MM, Brandell D (2017) Polycarbonates as alternative electrolyte host materials for solid-state sodium batteries. Electrochem Commun 77:58–61
12. Zhou D, Liu R, Zhang J, Qi X, He YB, Li B et al (2017) In situ synthesis of hierarchical poly(ionic liquid)-based solid electrolytes for high-safety lithium-ion and sodium-ion batteries. Nano Energy 33:45–54
13. Subba Reddy CV, Jin AP, Zhu QY, Mai LQ, Chen W (2006) Preparation and characterization of (PVP + $NaClO_4$) electrolytes for battery applications. Eur Phys J E 19:471–476
14. Aziz SB, Hamsan MH, Kadir MFZ, Karim WO, Abdullah RM (2019) Development of polymer blend electrolyte membranes based on chitosan: dextran with high ion transport properties for EDLC Application. Int J Mol Sci 20(13):3369
15. Kim JH, Min BR, Won J, Kim CK, Kang YS (2004) Structure and coordination properties of facilitated olefin transport membranes consisting of crosslinked poly(vinyl alcohol) and silver hexafluoroantimonate. J Polym Sci Part B Polym Phys 42:621–628
16. Gong SD, Huang Y, Cao HJ, Lin YH, Li Y, Tang SH, Wang MS, Li X (2016) A green and environment-friendly gel polymer electrolyte with higher performances based on the natural matrix of lignin. J Power Sources 307:624–633
17. Zhang J, Yue L, Kong Q, Liu Z, Zhou X, Zhang C, Xu Q, Zhang B, Ding G, Qin B, Duan Y, Wang Q, Yao J, Cui G, Chen L (2014) Sustainable, heat-resistant and flame-retardant cellulose-based composite separator for high-performance lithium ion battery. Sci Rep 4:1–8
18. Ng LS, Mohamad AA (2008) Effect of temperature on the performance of proton batteries based on chitosan-NH_4NO_3-EC membrane. J Memb Sci 325:653–657
19. Samsudin AS, Lai HM, Isa MIN (2014) Biopolymer materials based carboxymethyl cellulose as a proton conducting biopolymer electrolyte for application in rechargeable proton battery. Electrochim Acta 129:1–13
20. Shukur MF, Kadir MFZ (2014) Electrical and transport properties of NH_4Br-doped cornstarch-based solid biopolymer electrolyte. Ionics 21:111–124
21. Huang Y, Liu J, Zhang J, Jin S, Jiang Y, Zhang S, Li Z, Zhi C, Du G, Zhou H (2019) Flexible quasi-solid-state zinc ion batteries enabled by highly conductive carrageenan bio-polymer electrolyte. RSC Adv 9:16313–16319
22. Singh R, Bhattacharya B, Tomar SK, Singh V, Singh PK (2017) Electrical, optical and electrophotochemical studies on agarose based biopolymer electrolyte towards dye sensitized solar cell application. Measurement 102:214–219
23. Mindemark J, Lacey MJ, Bowden T, Brandell D (2018) Beyond PEO—alternative host materials for Li^+-conducting solid polymer electrolytes. Prog Polym Sci 81:114–143
24. Zhang L, Liu Z, Cui G, Chen L (2015) Biomass-derived materials for electrochemical energy storages. Prog Polym Sci 43:136–164
25. Kovalenko I, Zdyrko B, Magasinski A, Hertzberg B, Milicev Z, Burtovyy R, Luzinov I, Yushin G (2011) A major constituent of brown algae for use in high-capacity Li-ion batteries. Science 334(6052):75–79
26. Ling L, Bai Y, Wang Z, Ni Q, Chen G, Zhou Z, Wu C (2018) Remarkable effect of sodium alginate aqueous binder on anatase TiO_2 as high-performance anode in sodium ion batteries. ACS Appl Mater Interfaces 10:5560–5568
27. Smitha B, Sridhar S, Khan AA (2005) Chitosan-sodium alginate polyion complexes as fuel cell membranes. Eur Polym J 41:1859–1866
28. Yang JM, Wang NC, Chiu HC (2014) Preparation and characterization of poly(vinyl alcohol)/sodium alginate blended membrane for alkaline solid polymer electrolytes membrane. J Memb Sci 457:139–148
29. Kadokawa JI, Saitou S, Shoda SI (2005) Preparation of alginate-polymethacrylate hybrid material by radical polymerization of cationic methacrylate monomer in the presence of sodium alginate. Carbohydr Polym 60:253–258
30. Hu O, Chen G, Gu J, Lu J, Zhang J, Zhang X, Hou L, Jiang X (2020) A facile preparation method for anti-freezing, tough, transparent, conductive and thermoplastic poly(vinyl alcohol)/sodium alginate/glycerol organohydrogel electrolyte. Int J Biol Macromol 164:2512–2523
31. Czubacka E, Kruszynski R, Sieranski T (2012) The structure and thermal behaviour of sodium and potassium multinuclear compounds with hexamethylenetetramine. Struct Chem 23:451–459
32. Zhu H, Ströbele M, Yu Z, Wang Z, Meyer HJ, You X (2001) A blue luminescent di-2-pyridylamine cadmium complex with an unexpected arrangement of thiocyanate ligands: a supramolecular layered structure based on hydrogen bonds and π-π stacking interactions. Inorg Chem Commun 4:577–581
33. Chikte (Awade) D, Omanwar SK (2019) Synthesis and luminescence properties of novel NaSCN: xCe^{3+} phosphor. J Asian Ceramic Soc 7:350–354
34. Wan Y, Creber KAM, Peppley B, Tam Bui V (2006) Chitosan-based solid electrolyte composite membranes. I Preparation and characterization. J Memb Sci 280:666–674
35. Hodge RM, Edward GH, Simon GP (1996) Water absorption and states of water in semicrystalline poly(vinyl alcohol) films. Polymer 37:1371–1376
36. Malathi J, Kumaravadivel M, Brahmanandhan GM, Hema M, Baskaran R, Selvasekarapandian S (2010) Structural, thermal and electrical properties of PVA-LiCF3SO3 polymer electrolyte. J Non Cryst Solids 356:2277–2281
37. Aziz SB (2016) Role of dielectric constant on ion transport: reformulated Arrhenius equation. Adv Mater Sci Eng 2527013. https://doi.org/10.1155/2016/2527013
38. Hashmi SA, Chandra S (1995) Experimental investigations on a sodium-ion-conducting polymer electrolyte based on poly(ethylene oxide) complexed with NaPF6. Mater Sci Eng B 34:18–26

39. Sanders RA, Snow AG, Frech R, Glatzhofer DT (2003) A spectroscopic and conductivity comparison study of linear poly(N-methylethylenimine) with lithium triflate and sodium triflate. Electrochim Acta 48:2247–2253
40. Fuzlin AF, Samsudin AS (2020) Studies on favorable ionic conduction and structural properties of biopolymer electrolytes system-based alginate. Polym Bull. https://doi.org/10.1007/s00289-020-03207-2
41. Choi S, Kim JH, Kang YS (2001) Wide-angle X-ray scattering studies on the structural properties of polymer electrolytes containing silver ions. Macromolecules 34:9087–9092
42. Bhajantri RF, Ravindrachary V, Harisha A, Ranganathaiah C, Kumaraswamy GN (2007) Effect of barium chloride doping on PVA microstructure: positron annihilation study. Appl Phys A Mater Sci Process 87:797–805
43. Sikkanthar S, Karthikeyan S, Selvasekarapandian S, Pandi DV, Nithya S, Sanjeeviraja C (2015) Electrical conductivity characterization of polyacrylonitrile-ammonium bromide polymer electrolyte system. J Solid State Electrochem 19:987–999
44. Fuzlin AF, Bakri NA, Sahraoui B, Samsudin AS (2020) Study on the effect of lithium nitrate in ionic conduction properties based alginate biopolymer electrolytes. Mater Res Express 7(1):015902
45. Fromm KM (2008) Coordination polymer networks with s-block metal ions. Coord Chem Rev 252:856–885
46. Rivas BL, Maureira AE, Mondaca MA (2008) Aminodiacetic water-soluble polymer-metal ion interactions. Eur Polym J 44:2330–2338
47. De Santana H, Pelisson L, Diogo RJ, Zaia CTBV, Zaia DAM (2010) UV Radiation and the reaction between ammonium and thiocyanate under prebiotic chemistry conditions. J Serb Chem Soc 75:1381–1389
48. Salleh NS, Aziz SB, Aspanut Z, Kadir MFZ (2016) Electrical impedance and conduction mechanism analysis of biopolymer electrolytes based on methyl cellulose doped with ammonium iodide. Ionics 22:2157–2167
49. Ismayil VR, Bhajantri RF, Dhola PS, Sanjeev G (2015) Impact of electron-beam irradiation on free-volume related microstructural properties of PVA:NaBr polymer composites. Nucl Instruments Methods Phys Res Sect B Beam Interact with Mater Atoms 342:29–38
50. Mazuki NF, Fuzlin AF, Saadiah MA, Samsudin AS (2019) An investigation on the abnormal trend of the conductivity properties of CMC/PVA-doped NH4Cl-based solid biopolymer electrolyte system. Ionics 25:2657–2667
51. Kadir MFZ, Salleh NS, Hamsan MH, Aspanut Z, Majid NA, Shukur MF (2018) Biopolymeric electrolyte based on glycerolized methyl cellulose with NH4Br as proton source and potential application in EDLC. Ionics 24:1651–1662
52. Nakamura K, Nishimura Y, Hatakeyama T, Hatakeyama H (1995) Thermal properties of water insoluble alginate films containing di- and trivalent cations. Thermochim Acta 267:343–353
53. Siddaramaiah STMM, Ramaraj B, Lee JH (2008) Sodium alginate and its blends with starch: Thermal and morphological properties. J Appl Polym Sci 109:4075–4081
54. Swamy TMM, Ramaraj B, Siddaramaiah (2010) Sodium alginate and poly(ethylene glycol) blends: thermal and morphological behaviors. J Macromol Sci Part A Pure Appl Chem 47:877–881
55. Ojovan MI (2008) Viscosity and glass transition in amorphous oxides. Adv Condens Matter Phys 2008:1–23
56. Kim JH, Min BR, Won J, Kang YS (2003) Analysis of the glass transition behavior of polymer−salt complexes an extended configurational entropy model. J Phys Chem B 107(24):5901–5905
57. Chandra MVL, Karthikeyan S, Selvasekarapandian S, Pandi DV, Monisha S, Packiaseeli SA (2016) Characterization of high ionic conducting PVAc–PMMA blend-based polymer electrolyte for electrochemical applications. Ionics 22:2409–2420
58. Mohapatra SR, Thakur AK, Choudhary RNP (2009) Effect of nanoscopic confinement on improvement in ion conduction and stability properties of an intercalated polymer nanocomposite electrolyte for energy storage applications. J Power Sources 191:601–613
59. Sundaramahalingam K, Muthuvinayagam M, Nallamuthu N (2019) AC impedance analysis of lithium ion based PEO:PVP solid polymer blend electrolytes. Polym Sci Ser A 61:565–576
60. Boukamp BA (1986) A nonlinear least squares fit procedure for analysis of immittance data of electrochemical systems. Solid State Ionics 20:31–44
61. Saiful M, Rani A, Mohammad M, Sukor M, Ahmad A, Mohamed NS (2020) Novel approach for the utilization of ionic liquid - based cellulose derivative biosourced polymer electrolytes in safe sodium - ion batteries. Polym Bull. https://doi.org/10.1007/s00289-020-03382-2
62. Wagner JB, Wagner C (1957) Electrical conductivity measurements on cuprous halides. J Chem Phys 26:1597–1601
63. Okamoto Y, Tsuzuki S, Tatara R, Ueno K, Dokko K, Watanabe M (2020) High transference number of Na ion in liquid-state sulfolane solvates of sodium Bis(fluorosulfonyl)amide. J Phys Chem C 124(8):4459–4469
64. Slane S, Salomon M (1995) Composite gel electrolyte for rechargeable lithium batteries. J Power Sources 55:7–10
65. Ibrahim S, Ahmad A, Mohamed NS (2015) Characterization of novel castor oil-based polyurethane polymer electrolytes. Polymers 7:747–759
66. Isa KBM, Othman L, Hambali D, Osman Z (2017) Electrical and electrochemical studies on sodium ion-based gel polymer electrolytes. AIP Conf Proc 1877:040001
67. Subba Reddy CV, Sharma AK, Narasimha Rao VVR (2003) Conductivity and discharge characteristics of polyblend (PVP + PVA + KIO_3) electrolyte. J Power Sources 114:338–345